AIRFLOW REVERSALS IN HIGH-TEMPERATURE KILN DRYING OF *PINUS RADIATA* BOARDS. 2: DRYING OF A STACK OF BOARDS

PANG SHUSHENG

New Zealand Forest Research Institute,
Private Bag 3020, Rotorua, New Zealand

R. B. KEEY

Department of Chemical and Process Engineering,
University of Canterbury, Private Bag, Christchurch, New Zealand

J. C. F. WALKER

School of Forestry, University of Canterbury,
Private Bag, Christchurch, New Zealand

and T. A. G. LANGRISH

Department of Chemical Engineering,
University of Sydney, N.S.W. 2006, Australia

(Received for publication 30 June 1994; revision 30 September 1994)

ABSTRACT

A simplified description of drying kinetics was obtained from a rigorous mathematical model to describe the drying behaviour of a *Pinus radiata* D.Don board under high temperatures. Simplified characteristic drying curves, covering the falling-rate drying periods, were coupled with mass and heat balances over a control volume to determine the changes in air conditions (humidity and temperature) and local average moisture-content through the stack. This kiln-wide model was solved numerically to calculate the influence of airflow reversals under different strategies.

In drying of a kiln stack of sapwood boards with unidirectional airflow, the maximum difference in local average moisture-contents was about 0.4 kg/kg between 6 and 16 hours from the start of drying. Reversing the airflow every 4 or 8 hours only reduced the period in which the maximum difference in moisture content persisted, but no decrease in the greatest difference is predicted. This peak difference could be reduced to 0.3 kg/kg with airflow reversals every 3 hours. If the airflow was first reversed after 2 hours and again after 6 hours from the start of drying, the greatest difference in moisture content could be restricted to a little over 0.2 kg/kg. However, after 12 hours of drying, the various reversal strategies produced essentially similar profiles of moisture content, with

differences across the kiln between 0.1 to 0.2 kg/kg. In the drying of heartwood, differences were smaller, the maximum difference in local average moisture-content being less than 0.07 kg/kg with unidirectional airflow. This small difference could be reduced to less than 0.04 kg/kg when the first airflow reversal was performed within 4 hours of the start of drying.

Keywords: kiln-wide model; airflow reversals; humidity; local average moisture-content; *Pinus radiata.*

INTRODUCTION

In the high-temperature (HT) kiln drying of *Pinus radiata* timber, boards are generally piled in stacks to a width of 2.4 m or less and separated by stickers, usually 25 mm in thickness (Walker 1993). During drying, variations in air conditions (humidity, temperature, and air velocity) and consequently in wood moisture content take place across a stack. Without appropriate control of these variables, timber quality may be affected. As air flows over the boards, hot air transfers heat to the boards to evaporate moisture and at the same time carries away moisture as vapour from board surfaces. Thus, the dry-bulb temperature decreases and air humidity increases along the airflow direction. In addition, the external mean mass-transfer coefficient for individual boards decreases and tends towards an asymptotic value over the successive boards behind the front row, and so over the first row of boards the mean mass-transfer coefficient is significantly higher than that over the second and subsequent rows of boards (Kho *et al.* 1990; Langrish *et al.* 1993). Consequently, drying close to the inlet side of the stack with higher transfer rates is faster than near the downstream outlet side, where the air is becoming both cooler and more humid.

To mitigate this problem, airflow is normally reversed periodically by switching the fan direction. Reversing the direction of the airflow has the effect of enhancing drying both over the wetter zone of a stack and over the wetter section of each individual board. Meanwhile, drying of the drier parts of each board and at the previously drier air-inlet side of the stack is retarded. In this way, the drying differences between the two outer faces of the stack and between the two edges of individual boards (Pang *et al.* 1994) can be smoothed out to a certain extent. In practice, the frequency and length of the period between reversals are determined by trial and error. With different reversal strategies, there are variations in external conditions (temperature and humidity) through the drying schedule and consequently the variations in local average moisture content through a kiln stack are altered too. It is possible that some reversal policies are better than others in smoothing the moisture-content profiles.

Recently, a number of mathematical models have been developed to simulate the drying process in a single board (e.g., Pang *et al.* in press; Perré *et al.* 1988; Stanish *et al.* 1986). In these models, differential equations are set up from first principles to describe heat and mass-transfer rates within a board. By solving the resultant equations, temperature and moisture-content profiles can be predicted throughout the course of drying when the external conditions remain constant. However, coupling these equations with those to describe the varying air conditions within the kiln produces an equation set which is too complicated and computationally too slow for analysing commercial kiln behaviour (Kayihan 1993). Recently, a simplified model of drying kinetics has been advanced which enables a kiln-wide analysis to be undertaken relatively simply (Pang 1994; Pang & Keey 1994).

NOMENCLATURE

a	exposed surface per unit volume of dryer (m^2/m^3)
c	coefficient in Equation (10)
C_{PG}	specific heat of the air (J/kg·K)
C_{PV}	specific heat of water vapour (J/kg·K)
f	relative drying-rate function
f_1	relative drying rate in the second period of drying
f_2	relative drying rate in the third period of drying
$f^{(1)}$	relative drying-rate function in the second period of drying
$f^{(2)}$	relative drying-rate function in the third period of drying
G	specific dry gas rate ($kg/m^2 \cdot s$)
H_{wv}	heat of vaporization of water (J/kg)
K_0	mass-transfer coefficient based on humidity potential ($kg/m^2 \cdot s$)
T_G	dry-bulb temperature of the air at positions downstream (K)
X	average moisture-content (kg/kg)
X_0	initial moisture content of wood (kg/kg)
X_1	average moisture-content at the first critical point (kg/kg)
X_2	average moisture-content at the second critical point (kg/kg)
X_e	equilibrium moisture content (kg/kg)
Y_G	humidity of the air at any position across a stack (kg/kg)
Y_G^0	humidity of the air at the air intake (kg/kg)
Y_S	humidity of the air when saturated at wet-bulb temperature (kg/kg)
z	distance from air intake (m)

Greek Characters

α	ratio of the first critical drying rate to the second critical drying rate
α_H	ratio of the radiative heat to the conductive heat
ε	voidage of the board stack in a kiln
ρ_S	basic density of wood (kg/m^3)
φ	humidity-potential coefficient
Φ	normalised or characteristic moisture content
$\Phi^{(1)}$	normalised moisture content in the first period and the second periods of drying
$\Phi^{(2)}$	normalised moisture content in the third period of drying
Π	dimensionless parameter for humidity potential
ζ	dimensionless parameter for distance
θ	dimensionless parameter for drying time
γ	dimensionless parameter for temperature
τ	drying time (s)

DRYING-RATE CURVES FROM A RIGOROUS SINGLE-BOARD MODEL

A Heartwood Board

An example of the drying rate curve generated from the mathematical model derived by Pang *et al.* (1994) is shown in Fig. 1 for high-temperature drying of a heartwood board. In

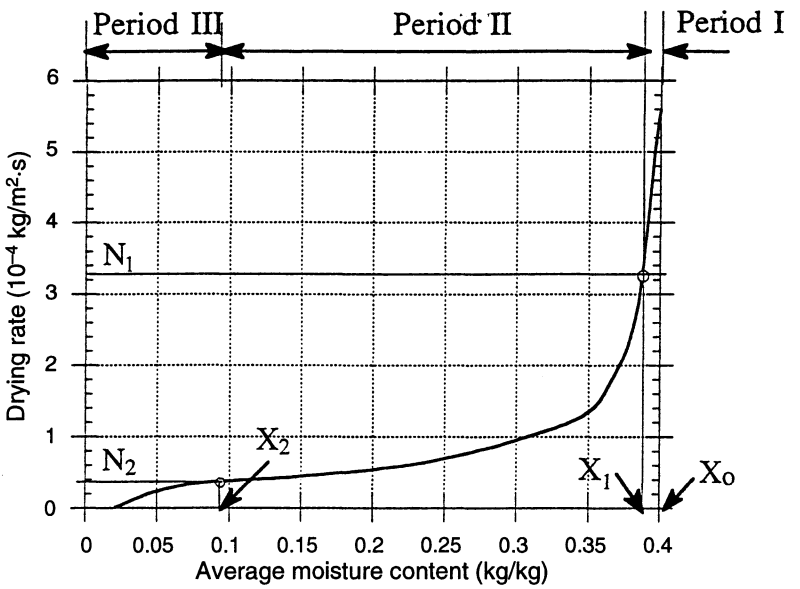

FIG. 1–The drying rate curve for a heartwood board of *Pinus radiata* calculated from the rigorous model (Pang 1994). Dry-bulb temperature 120°C; wet-bulb temperature 70°C; air velocity 5 m/s.

this example, the dry-bulb/wet-bulb temperatures were 120°/70°C and the air velocity was 5 m/s. The whole process of drying can be divided into three periods. Initially, the surface temperature of the board rises just above the wet-bulb temperature and liquid moisture at the surface evaporates to diffuse into the airstream. At this time the drying rate is at maximum, but as there is no liquid water flow towards the surface, an evaporative front quickly withdraws into the board. In this first period, the external conditions are dominant, but very quickly the influence of internal resistance to moisture vapour transport becomes significant and the drying rate drops sharply. By the end of this period (some 5–15 minutes from the start of drying) the evaporative front has withdrawn a short distance from the surface (about 0.5 mm) and the internal transfer begins to control the drying. The subsequent course of drying can be represented by two falling-rate periods—in this paper referred to as period two and period three respectively. In period two, the evaporative front continues to recede into the board at a rate which is not primarily determined by the external conditions. This period may last 8 to 14 hours according to the drying temperature. Finally, once the evaporative front reaches the mid-plane of the board, drying is dominated by bound water diffusion. This is the third period of drying. Since the duration of the first period is so short as to be insignificant, it is not distinguished here from the second period except that the drying rate at the end of the first period is used as the initial value for the analysis. Therefore, the whole drying process can be described by two falling-rate periods.

In this analysis, the first critical point is defined as the time when the evaporative front has withdrawn to a short distance from the surface (about 0.5 mm), when the internal resistance to moisture vapour flow becomes dominant. The corresponding mean moisture-content for the whole board at this time is X_1 and the drying rate is N_1. The second critical

point is defined when the front has reached the mid-plane of the board, and the corresponding mean moisture-content and drying rate are X_2 and N_2 respectively.

A Sapwood Board

The proposed mathematical model (Pang *et al.* 1994) can also be used to simulate drying of a sapwood board (Fig. 2). In the calculation, the same external conditions as those for heartwood were used. From the drying-rate curve, the drying process can also be divided into three periods:

(1) The evaporative front remains near the exposed surface. As the material is heated in the early stages of drying, the drying rate increases initially, then rises to a maximum and remains relatively constant. This period is the first period and a constant drying rate will be assumed in the further analysis.

(2) The evaporative front recedes into the board and the drying-rate curve is concave in form. This period is the first falling-rate period, but the second period for the whole drying process.

(3) Bound water diffusion and moisture vapour movement control. The drying rate falls rapidly with diminishing moisture content until the drying rate is virtually zero as the timber approaches equilibrium with the airstream. This period is the second falling-rate period—the third period of drying.

The first period of drying for sapwood is far more extensive than for heartwood (Fig. 1 and 2). Once the board has been warmed up, the drying rate remains at a relatively high level.

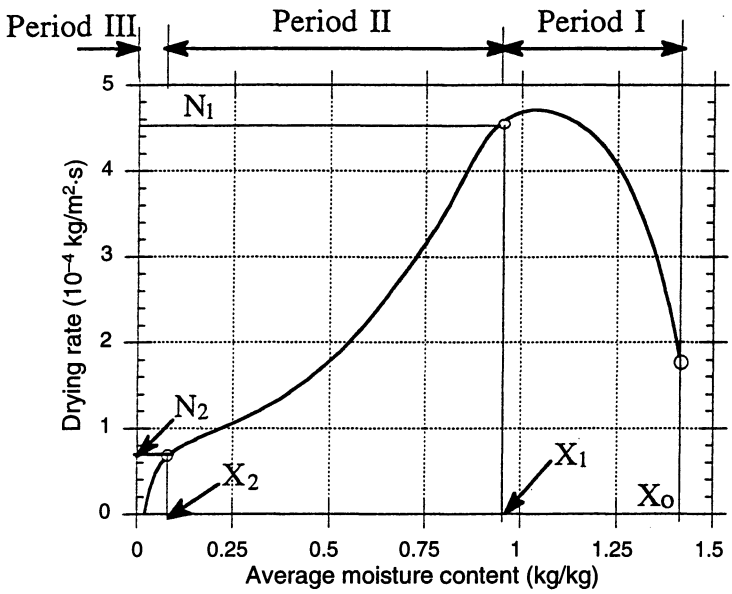

FIG. 2–The drying rate curve for a sapwood board of *Pinus radiata* calculated from the rigorous model (Pang 1994). Dry-bulb temperature 120°C; wet-bulb temperature 70°C; air velocity 5 m/s.

In the second period the drying rate for sapwood is higher than that for heartwood because of the liquid flow towards the evaporative front.

For sapwood drying, we define the first critical point as that when the evaporative front starts to recede into the wood leaving the thin drying layer. This is when the second period starts. Similarly, we define the second critical point as that when the second period ends and the third period starts.

DRYING KINETICS

Keey (1978) described streamwise variations of humidity potential, drying rate, and moisture content in batch dryers by employing an idea put forward earlier by van Meel (1958). It was proposed that drying rate curves for a specific material were geometrically similar, irrespective of the external conditions. This has become known as *the characteristic drying curve*, which describes a functional relationship between a relative drying rate and a normalised moisture content. If the function is known, one can calculate changes of drying rate and moisture content through the dryer by solving an equation set derived from mass and energy conservation over a control zone in the kiln. Since characteristic drying curves differ with factors such as the shape of the material and the configuration in a dryer, the drying curve is usually determined from laboratory experimental data. By contrast, we obtained characteristic drying curves from the numerical results of the rigorous mathematical model, and thus extensive drying tests could be avoided (Pang 1994; Pang & Keey 1994). Dual characteristic drying curves could be developed to describe the two falling-rate periods, whereas normally a single characteristic curve is fitted to the data over the whole falling-rate drying process.

With an impermeable *P. radiata* heartwood board, drying is essentially dominated by periods two and three, i.e., the first period lasting 5–15 minutes is ignored. Two separate characteristic drying curves in these two periods have been derived to express drying behaviour over the whole process. For sapwood, the drying process consists of three periods: a relatively constant period and two falling-rate periods. The characteristic drying curves for each period have been examined by Pang (1994) and Keey & Pang (in press).

MODELLING OF AVERAGE MOISTURE-CONTENT AND TEMPERATURE PROFILES THROUGH A STACK OF BOARDS

If the kiln is assumed to be well-insulated and the air to be distributed evenly over the boards, then only streamwise variations need to be considered as the spanwise variations are small in comparison (Ashworth 1977; Keey 1992). There is some experimental evidence to suggest that in well-designed kilns the airflow can be almost uniformly distributed through each duct surrounded by two board layers and stickers (Wiedeman *et al.* 1989). This assumption should be valid when the boards are neatly stacked and "boxed" (Fig. 3). In principle, non-uniformity of flow can be taken into account by considering the kiln to consist of a series of uniformly ventilated ducts in parallel; in a similar way, Keey & Wu (1989) analysed the behaviour of continuous dryers which were being fed unevenly with moist material. Further, the mass-transfer coefficient over a single board is considered to be the distance-averaged value over this board. The local moisture content predicted is thus the mean value over each board.

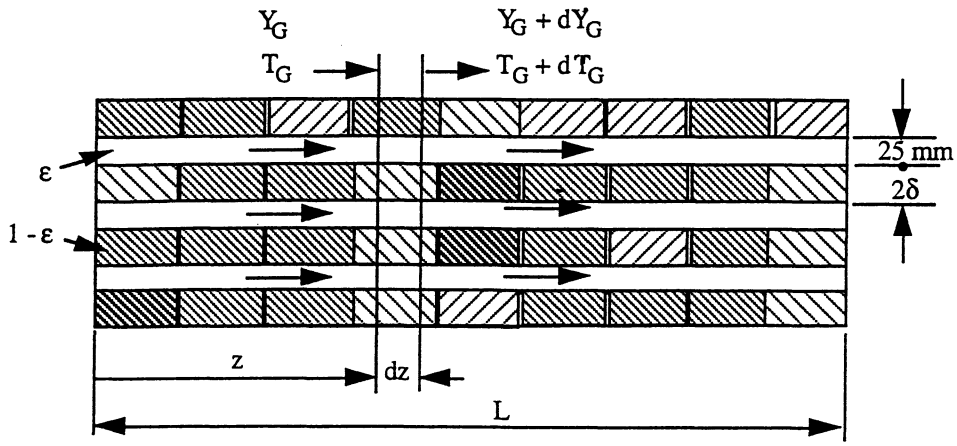

FIG. 3–Schematic diagram of part of a well-constructed timber stack.

Constitutive Equations for Moisture Mass Balance

By considering moisture balances over an infinitesimally short distance *dz* within the kiln (Fig. 3), a set of differential equations can be developed describing the conditions at any position in the kiln. In non-dimensional form, these equations become:

$$\frac{\partial \Phi}{\partial \theta} = \frac{\partial \Pi}{\partial \zeta} \tag{1}$$

$$-\frac{\partial \Phi}{\partial \theta} = \Pi f \tag{2}$$

in which Π, Φ, θ, and ζ are the dimensionless parameters for humidity potential, moisture content, elapsed time, and distance from the air inlet. These equations have the same form as proposed by Keey (1978) and Ashworth (1977) except that the new functions of $f^{(1)}$ and $f^{(2)}$ are used to replace the single relative drying-rate function f for the second period and the third period of drying as follows:

$$f = f^{(1)} = [f_1(1-\alpha) + \alpha] \tag{3}$$

where $X_1 > X > X_2$, f_1 is the value of the relative drying rate during the second period of drying, and α is the coefficient of proportionality between the first and second critical drying rates.

Whenever $X_2 > X > X_e$,

$$f = f^{(2)} = \alpha f_2 \tag{4}$$

in which f_2 is the relative drying rate in the third period of drying. Further, new dimensionless parameters for moisture content, $\Phi^{(1)}$ and $\Phi^{(2)}$, are used for the corresponding periods of drying such that

$$\Phi^{(1)} = \frac{X - X_1}{X_1 - X_2} \tag{5}$$

$$\Phi^{(1)} = \frac{X - X_e}{X_2 - X_e} \tag{6}$$

The other dimensionless parameters which appear in Equations (1) and (2) for the drying of the boards are defined as follows:

(i) The relative distance along the dryer:

$$\zeta = \frac{K_0 \varphi a}{G} z \tag{7}$$

which is the number of transfer units or extensiveness in the airflow direction.

(ii) The relative drying time:

$$\theta=\theta_1 = \frac{K_0 \varphi a (Y_S - Y_G^0)}{\rho_S (1-\varepsilon)(X_1 - X_2)} \tau, \text{ when } X_1 > X > X_2$$

$$\theta=\theta_2 = \frac{K_0 \varphi a (Y_S - Y_G^0)}{\rho_S (1-\varepsilon)(X_2 - X_e)} \tau, \text{ when } X_2 > X > X_e \tag{8}$$

The relative time has the meaning of the ratio of the maximum moisture-transfer rate to the moisture load between the critical points.

(iii) The humidity potential relative to the value at the air inlet:

$$\Pi = \frac{Y_S - Y_G}{Y_S - Y_G^0} \tag{9}$$

In Equations (5) to (9), each variable is defined in the nomenclature.

Constitutive Equations for Heat Conservation

In kiln drying of a stack of boards, the hot air provides convective heat to evaporate moisture from the boards. Additional heat received by the boards may come from the kiln walls or the warm air by radiation. On considering heat conservation over a short distance dz as shown by Pang (1994) and Keey & Pang (in press), the change in temperature with humidity potential becomes:

$$\frac{\partial \gamma}{\partial \Pi} = \frac{1}{c - \Pi} = \frac{1}{[Y_S + \frac{C_{PG}}{C_{PV}}] / (Y_S - Y_G^0) - \Pi} \tag{10}$$

where c is a constant and γ is a non-dimensional temperature given by

$$\gamma = \frac{(1 + \alpha_H) C_{PV} T_G}{H_{wv}} \tag{11}$$

In other words, the rate at which the temperature changes with the humidity potential is almost constant since the coefficient c is much greater than Π and varies only slightly over the normal range of air conditions in a kiln. This indicates that the temperature profile will be similar to that of humidity potential.

SIMULATION RESULTS FOR UNIDIRECTIONAL AIRFLOW AND FOR AIRFLOW REVERSALS

The stack of timber, in effect, presents a series of ducts for the air to pass through at right-angles to the flat surfaces of the boards. These ducts are not smooth-sided, but are interrupted by very small edge gaps between adjacent boards. Although these gaps, which inevitably occur as boards shrink and twist, may be only between 1 and 5 mm in width, they have a remarkable influence on the airflow pattern, and hence the mass-transfer coefficients. In the previous paper (Pang *et al.* 1994), the profile of the local averaged external mass-transfer

coefficient with distance along the airstream through a kiln stack was presented, based on work by Kho *et al.* (1990).

Using the board-average values of the mass-transfer coefficients, the local average moisture-contents can be calculated for different stages of drying with unidirectional airflow by employing the kiln-wide model as described in detail elsewhere (Pang 1994; Keey & Pang in press) (see, for example, Fig. 4a). The calculated results for sapwood drying from each reversal strategy (Pang *et al.* 1994) are given in Fig. 4b–4f. The changes in local average moisture-contents with distance along the airstream from the original leading edge are presented for different stages of drying. To describe the uneven distribution of local average moisture-contents across a kiln stack, the maximum differences through the stack with drying time are given in Fig. 5 and 6. In Fig. 5 different time intervals for uniform airflow reversals are compared with unidirectional airflow; in Fig. 6 the results of reversing the airflow only once after 4 hours of drying are compared with reversals every 4 hours, and another curve is plotted with reversals after 2 and 6 hours from the start of drying. External conditions and wood properties used in the calculations are set out in Table 1.

TABLE 1–Values of the parameters used in the simulation of high-temperature drying of a single *Pinus radiata* board.

Parameters	Heartwood	Sapwood
Wood density, ρ_s (kg/m^3)	377	450
Initial moisture content, X (kg/kg)	0.40	1.40
First critical moisture content, X_1 (kg/kg)	0.4	0.94
Second critical moisture content, X_2 (kg/kg)	0.088	0.093
Equilibrium moisture content, X_e (kg/kg)	0.022	0.022
Board dimension (mm)	100 × 50	100 × 50
Width of the stack (m)	2.4	2.4
Void fraction of the stack, ε (m^3/m^3)	0.333	0.333
Air humidity saturated at wet-bulb temperature, Y_s (kg/kg)	0.277	0.277
Air humidity at air intake, Y^0_G (kg/kg)	0.246	0.246
Dry air specific rate, G (kg/m^2·s)	1.471	1.471

A similar evaluation for heartwood drying is given in Fig. 7–9. As the initial moisture content for heartwood is much lower than that for sapwood, the differences in local average moisture contents are much less than for sapwood at the same elapsed time of drying.

DISCUSSION

Sapwood

Before drying, moisture content is initially assumed to be the same throughout the kiln stack. As drying proceeds, the boards at the air intake dry faster than those further along the airstream. When the airflow direction is reversed, however, external conditions through the stack are reversed and the local drying rates follow this change. As a result, the boards near the new air intake (the old air offtake) dry faster that those close to the new air offtake (the old air intake). This process is repeated whenever the airflow is reversed. Hence, after each

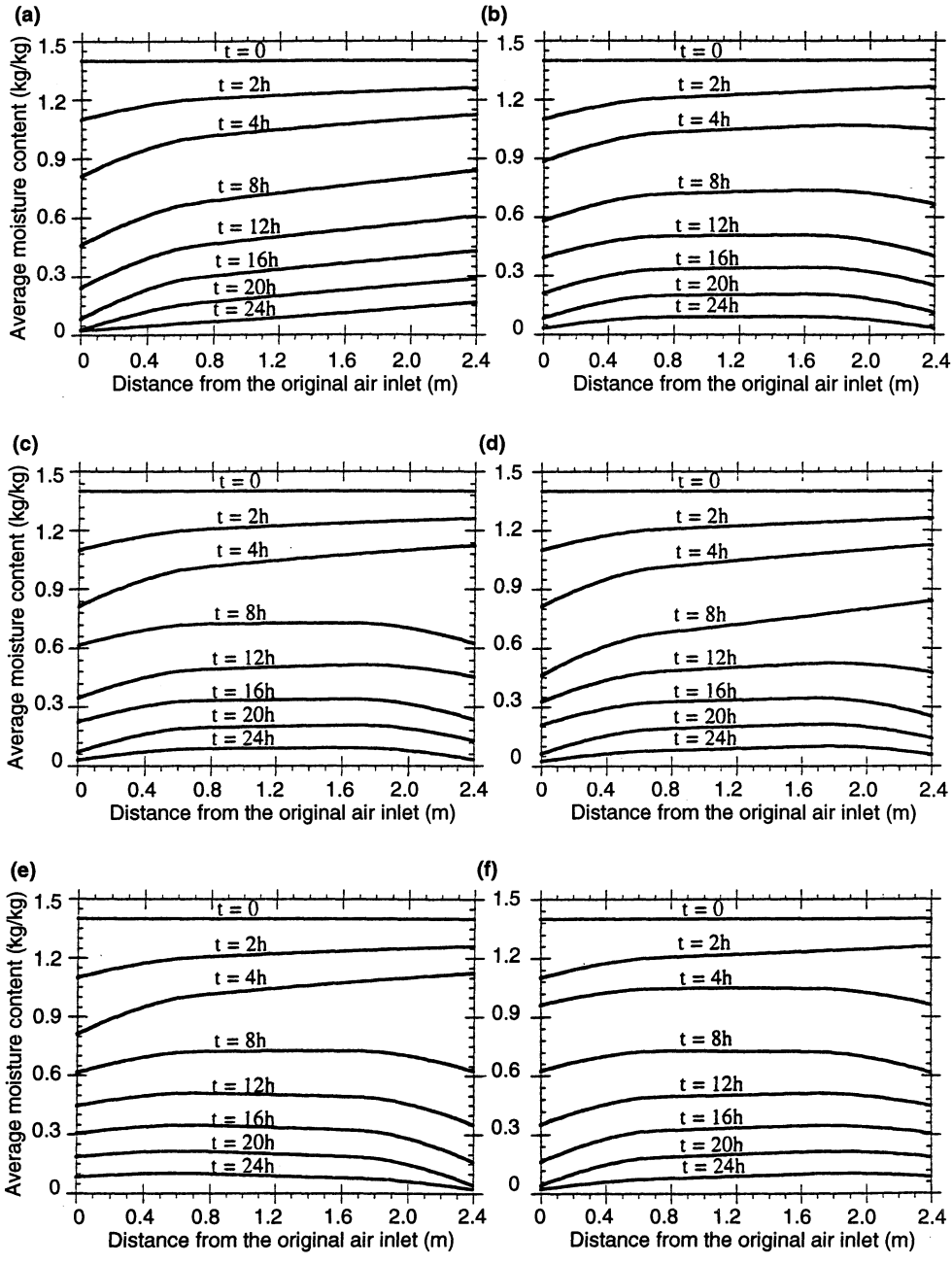

FIG. 4–Distribution of local average moisture-content through a kiln stack of sapwood boards with different airflow strategies. Dry-bulb/wet-bulb temperatures 120°/70°C; air velocity 5 m/s. (a) Unidirectional airflow; (b) airflow reversed every 3 hours; (c) airflow reversed every 4 hours; (d) airflow reversed every 8 hours; (e) airflow reversed only once; (f) airflow reversed after 2 and after 6 hours.

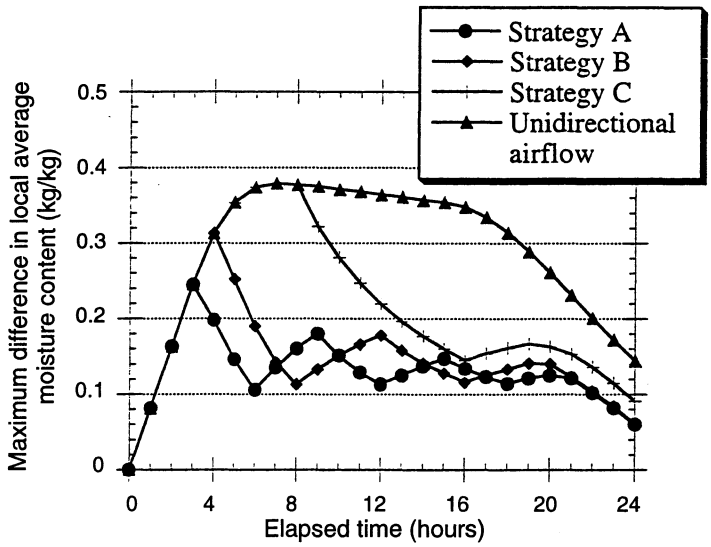

FIG. 5–Comparison of maximum differences in local average moisture content between sapwood boards in a 2.4-m-wide stack, with different time intervals for airflow reversals and with unidirectional airflow. A = airflow reversed every 3 hours; B = airflow reversed every 4 hours; C = airflow reversed every 8 hours.

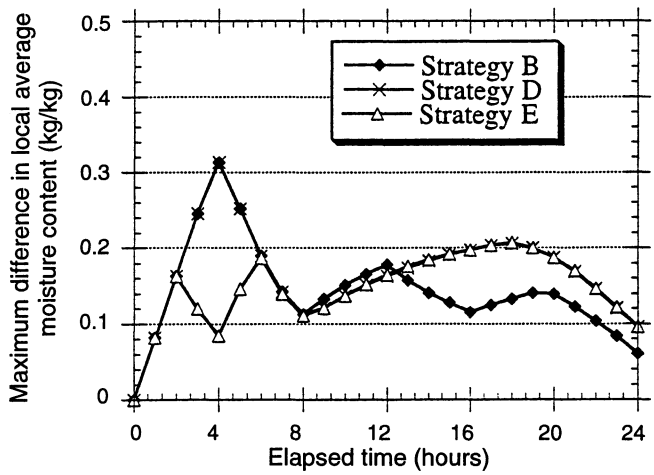

FIG. 6–Comparison of maximum differences in local average moisture content between sapwood boards in a 2.4-m-wide stack, with airflow reversals every 4 hours (B), only once after 4 hours (D), and only twice after 2 and 6 hours (E).

airflow reversal, the average moisture-contents at both sides of the stack achieve essentially similar values and the early differences between them can be smoothed out. Soon after the first airflow reversal, the mid-area in the kiln stack becomes the wettest zone since the external conditions over this area are virtually unchanged, even though the airflow may have

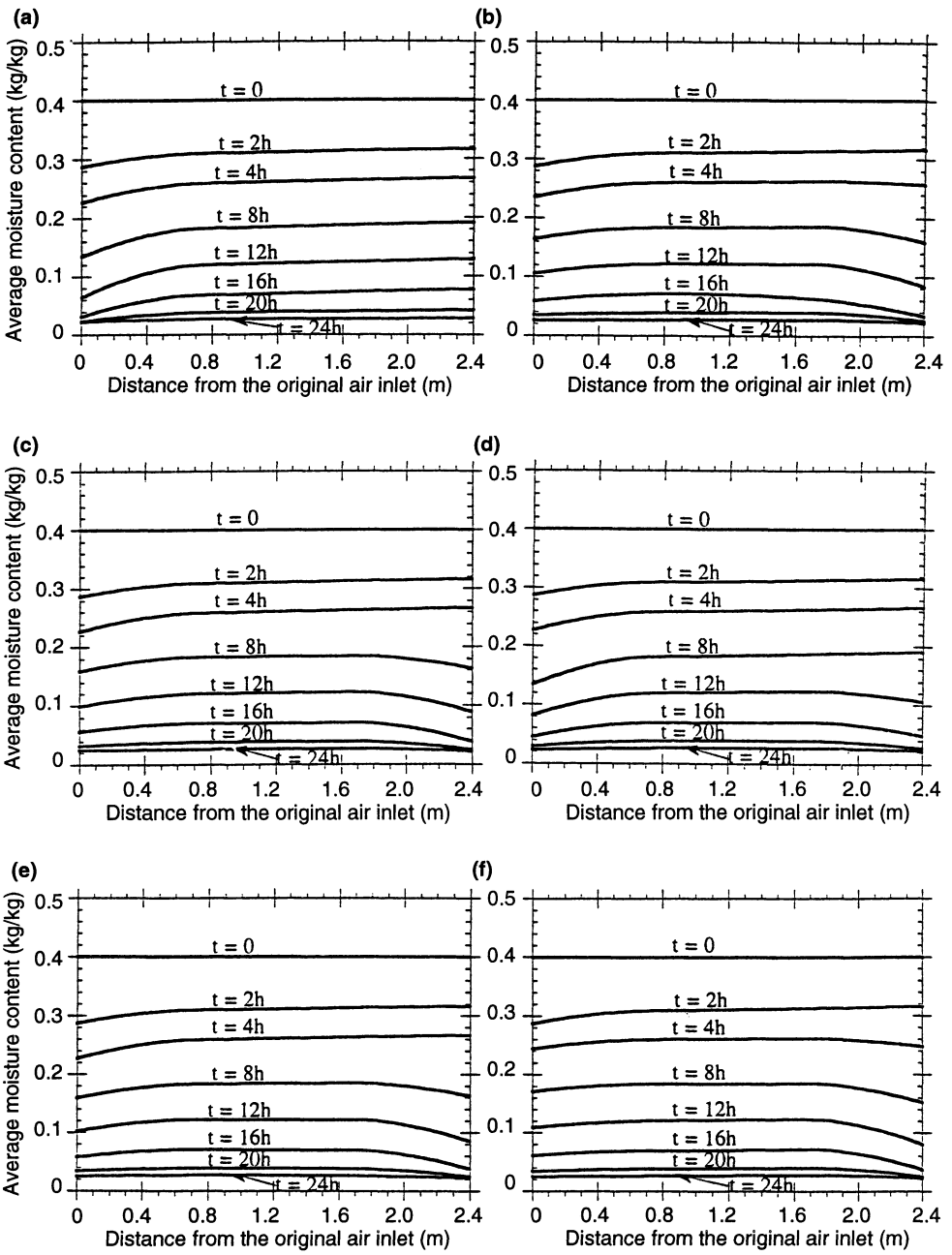

FIG. 7–Distribution of local average moisture content through a kiln stack of heartwood boards with different airflow strategies. Dry-bulb/wet-bulb temperatures 120°/70°C; air velocity 5 m/s. (a) Unidirectional airflow; (b) airflow reversed every 3 hours; (c) airflow reversed every 4 hours; (d) airflow reversed every 8 hours; (e) airflow reversed only once; (f) airflow reversed after 2 and after 6 hours.

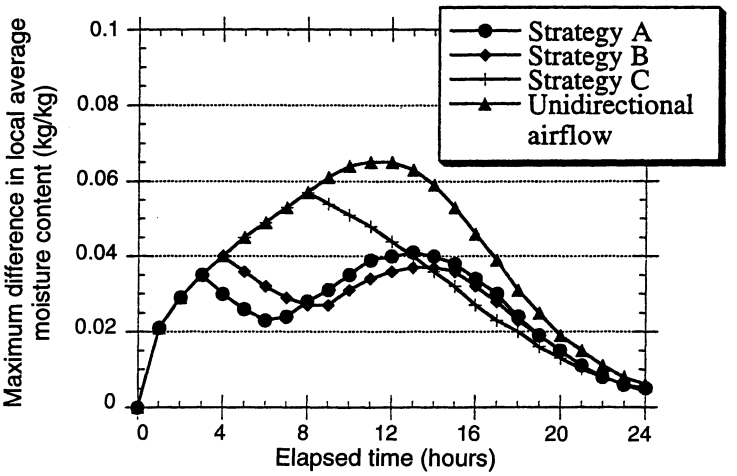

FIG. 8–Comparison of maximum differences in local average moisture content between heartwood boards in a 2.4-m-wide stack, with different time intervals for airflow reversals and with unidirectional airflow. A = airflow reversed every 3 hours; B = airflow reversed every 4 hours; C = airflow reversed every 8 hours.

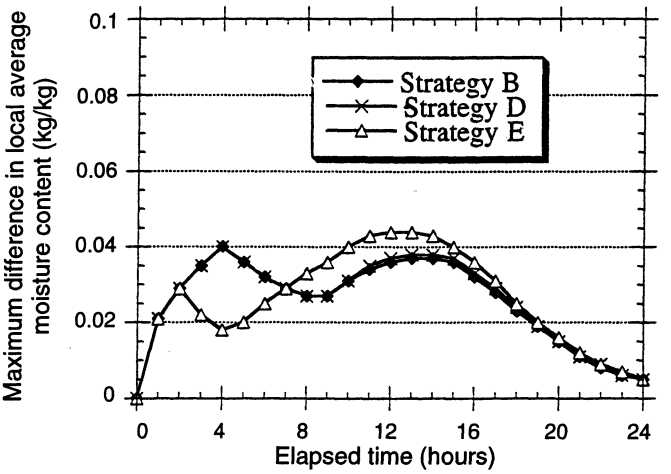

FIG. 9–Comparison of maximum differences in local average moisture content between heartwood boards in a 2.4-m-wide stack, with airflow reversals every 4 hours (B), only once after 4 hours (D), and only twice after 2 and 6 hours (E).

been reversed several times. Airflow reversals thus significantly influence the magnitude of the transfer rates only near both ends of the stack where the humidity potential is effectively changed by switching the airflow direction.

With unidirectional airflow, the maximum differences in local average moisture content across a stack are in the range 36% to 38% moisture content (m.c.) during 6 to 16 hours of drying (Fig. 5). With airflow reversals every 8 hours, the peak value cannot be reduced but

the duration of the peak value is reduced from 10 hours to 4 hours. Maximum differences in local average moisture content are reduced to 30% m.c. with 4-hour reversals and to 25% m.c. with 3-hour reversals. These peak values occur just before the first reversal and are not long-lasting. With further reversals, the maximum difference in moisture content remains between 10% m.c. and 20% m.c. without significant variations between different reversal strategies. This means that the first reversal is critical to minimise uneven distribution of local average moisture content through a kiln stack of sapwood boards.

After 20 hours of drying, the maximum differences in local average moisture content for each strategy of uniform reversals are between 12% and 16% m.c., while the actual values of the average moisture contents across a kiln stack vary from 6% to 22% m.c.. With another 4 hours of drying, the maximum difference in local average moisture content can be reduced to less than 8% m.c. Since at this stage of drying, the driest zones at both sides of the stack approach the equilibrium value, the moisture contents across the stack fall in a range of 3% to 11% m.c. The range in average moisture contents is: 3.0% to 9% m.c. for reversals every 3 hours, 3.0% to 9.1% m.c. for reversals every 4 hours, and 2.4% to 10.3% m.c. for reversals every 8 hours. This range emphasises the difficulty of obtaining acceptable final moisture content for wood products solely by a batch-drying process. In practice, reconditioning is applied immediately after high-temperature drying. This serves the dual purpose of relieving drying stresses and helping to reduce moisture content variation within and between boards.

The single reversal strategy can produce a result essentially similar to that with 4-hourly reversals within the first 12 hours (Fig. 6). However, after this time the maximum difference in moisture content with the single reversal strategy becomes greater. After 24 hours of drying, the local average moisture contents with the single reversal strategy vary from 2.2% to 11% m.c., compared with 3% to 9% m.c. with reversals every 4 hours. When the airflow is reversed only twice after 2 and 6 hours, the maximum difference in moisture content during the initial stages of drying can be further reduced from those observed with uniform reversals to below 0.2 kg/kg. After 8 hours, the moisture-content variations are virtually the same as those with a single airflow reversal after 4 hours.

Heartwood

With the unidirectional airflow, the greatest moisture content difference is 6.5% m.c. after 10 hours of drying. For drying with uniform airflow reversals, this value is reduced to 5.5% m.c. for reversals every 8 hours, and to 4.0% m.c. for reversals every 3 or 4 hours. With reversals every 4 or 8 hours, the greatest differences in local average moisture content occur just before the first reversal, while with the reversals every 3 hours the greatest non-uniform distribution occurs between 8 and 14 hours from the start of drying. After 16 hours of drying the greatest differences with each uniform reversal strategy are reduced to less than 3.8% m.c., with the actual average moisture content ranging from 3.3% to 7.1%. A single airflow reversal after 4 hours has virtually the same effect as uniformly spaced reversals every 4 hours, whereas the results with reversals after 2 and 6 hours are similar to those with reversals every 3 hours.

CONCLUSIONS AND RECOMMENDATIONS

Using the board-average, mass-transfer coefficient profile, we have predicted the variations in local average moisture-contents and changes in external condition (temperature

and humidity) through a kiln-stack of *P. radiata* boards during HT drying. When the air flows in one direction only, the drying rates over the boards close to the air inlet side are much higher than those near the air outlet, resulting in significant variations in local average moisture-content. With airflow reversals, these variations can be reduced and more-uniform moisture-content profiles can be obtained. This should reduce the number of drying-related defects.

On the basis of our calculations, we make the following recommendations:

- The first reversal of the airflow is critical to reduce the maximum differences in average moisture-content through a kiln-stack. The maximum difference in average moisture-content occurs just before the airflow is first reversed when drying lasts longer than 2 hours. Therefore, the first reversal after 2 hours from the start of drying can smooth out the peak value in moisture-content difference.
- Frequent reversals are not necessary. A reversal after 2 hours and another after 6 hours from the start of drying may be enough to give an adequate degree of uniformity in temperature and moisture-content profiles within boards and within a kiln stack.

The calculations presented in this paper were based on a kiln-wide simulation model (Pang 1994; Keey & Pang in press). The predictions from this model have been qualitatively confirmed by kiln operators. However, further quantitative verification by drying tests in either a commercial kiln or pilot-scale kiln will be necessary.

ACKNOWLEDGMENTS

This work is supported by the New Zealand Public Good Science Fund (UOC 302 and 406). Pang Shusheng also acknowledges financial support from New Zealand FRST fund (CO4415) in preparing this paper. The single-board drying experiments were carried out at the New Zealand Forest Research Institute, Rotorua. The authors wish to thank Mr W.R.Miller, Mr A.N.Haslett, and Mr I.G.Simpson for the arrangement and for their help in conducting the drying tests. We also appreciate the helpful discussions with Dr J.A.Kininmonth of Winsor Engineering Group Ltd, Rotorua, in preparing this paper.

REFERENCES

ASHWORTH, J.A. 1977: The mathematical simulation of the batch drying of softwood timber. Ph.D. Thesis, University of Canterbury, New Zealand.

KAYIHAN, F. 1993: Adaptive control of stochastic batch lumber kilns. *Computers Chemical Engineering 17(3)*: 265–73.

KEEY, R.B. 1978: "Introduction to Industrial Drying Operations". Pergamon Press, Oxford. 376 p.

——1992: "Drying of Loose and Particulate Materials". Hemisphere Publishing Co., New York. 504 p.

KEEY, R.B.; PANG SHUSHENG: The high-temperature drying of softwood boards: a kiln-wide model. *Transactions IChemE Series A* (in press).

KEEY, R.B.; WU YUAN 1989: The influence of unevenness of the wool mat on the drying of loose wool. *Chemical Engineering Processing 26*: 127–37.

KHO, P.C.S.; KEEY, R.B.; WALKER, J.C.F. 1990: The variation of local mass-transfer coefficients in streamwise direction over in-line, blunt slabs. *Proceedings of Chemeca'90 Conference, Auckland, New Zealand, Vol.1*: 348–55.

LANGRISH, T.A.G.; KEEY, R.B; KHO, P.C.S.; WALKER, J.C.F. 1993: Time-dependent flow in arrays of timber boards: flow visualisation, mass-transfer measurement and numerical simulation. *Chemical Engineering Science 48*: 2211–23.

PANG SHUSHENG 1994: High-temperature drying of *Pinus radiata* boards in a batch kiln. Ph.D. Thesis, University of Canterbury, Christchurch, New Zealand.

PANG SHUSHENG; KEEY, R.B. 1994: The drying kinetics of an impermeable heartwood board of *Pinus radiata* at elevated temperatures. *Proceedings of IDS '94, 9th International Drying Symposium, Brisbane, Australia, B*: 1273–82.

PANG SHUSHENG; LANGRISH, T.A.G.; KEEY, R.B.: Moisture movement in softwood timber at elevated temperatures. *Drying Technology 14(7)* (in press).

PANG SHUSHENG; KEEY, R.B.; LANGRISH, T.A.G.; WALKER, J.C.F. 1994: Airflow reversals in the high-temperature kiln drying of *Pinus radiata* boards. 1: Drying of a single board. *New Zealand Journal of Forestry Science 24(1)*: 83–103.

PERRE, P.; FOHR, J.R.; ARNAUD, G. 1988: A model applied to softwood: The effect of gaseous pressure below the boiling point. *Proceedings of the 6th International Drying Symposium, Versailles*: 279–86.

STANISH, M.A.; SCHAJER, G.S.; KAYIHAN, F. 1986: A mathematical model of drying for hygroscopic porous media. *Association of International Chemical Engineers Journal 32(8)*: 1301–11.

VAN MEEL, D.A. 1958: Adiabatic convective batch drying with recirculation of air. *Chemical Engineering Science 9*: 36–44.

WALKER, J.C.F. 1993: "Primary Wood Processing: Principles and Practice". Chapman and Hall, London. 595 p.

WIEDEMAN, H.G.R.; NASSIF, N.M.; GOSTELOW, J.P. 1989: Study of the air flow profile inside a timber drying kiln. Pp.693–701 *in* Keey, R.B. (Ed.) "Heat and Mass Transfer '89", Proceedings of the 4th Australasian Conference on Heat and Mass Transfer, Christchurch, New Zealand.